Reconciliation of rocket-based magnetic field measurements in the equatorial electrojet with classical collision theory

M. C. Kelley,[1] R. R. Ilma,[1] and V. Eccles[2]

Received 20 July 2011; revised 9 November 2011; accepted 10 November 2011; published 14 January 2012.

[1] We provide an explanation for a long-standing (more than 35 years) discrepancy between theory and rocket experiments concerning the peak height of the electrojet current and the magnitude of magnetic field perturbation. The arbitrary correction of the electron-neutral collision frequency by a factor of 4, which has been used to explain these problems, is not necessary if the field line–integrated conductivities are used. Recent research using ground-based magnetometers and CHAMP have also used this constant connection to classical collision theory. These methods arbitrarily change the electron-neutral collision frequency. A field line–integrated theoretical study of the electrojet by G. Haerendel and J. V. Eccles, implemented in this paper, explains the height of the electrojet using classical collision frequency. Furthermore, we argue that since the correction factor is independent of the driving electric field, it is unlikely that anomalous electron collision frequency due to a nonlinear plasma instability (gradient drift) is involved.

Citation: Kelley, M. C., R. R. Ilma, and V. Eccles (2012), Reconciliation of rocket-based magnetic field measurements in the equatorial electrojet with classical collision theory, *J. Geophys. Res.*, *117*, A01311, doi:10.1029/2011JA017020.

1. Introduction

[2] The equatorial electrojet (EEJ), an intense current at the magnetic equator, has been studied for nearly a century and is a rich source of information on conditions in the ionosphere as well as the character of nonlinear development of plasma instabilities. *Richmond* [1973] summarized rocket magnetic field measurements made in the equatorial electrojet and compared them with model calculations, as reproduced in Figure 1. Notice that the altitudinal peak in the magnitude of the predicted current is higher than the data show. These results were obtained with experiments off the coast of Peru and were verified off Brazil by *Pfaff et al.* [1997]. *Gagnepain et al.* [1977] looked at many different models and found that to fit the data, they had to arbitrarily increase the electron-neutral collision frequency (ν_{en}) by a factor of 4.

[3] *Alken and Maus* [2007] developed an EEJ model on the basis of electrojet currents inferred from the Challenging Minisatellite Payload (CHAMP) magnetic field measurements that has been successfully validated with about six years of concurrent observations using the Jicamarca Unattended Long-term investigations of the Ionosphere and Atmosphere (JULIA) radar. The 50 MHz radar measures the plasma velocity perpendicular to the magnetic field at Jicamarca, Peru. CHAMP was in a circular polar orbit at an altitude of 474 km. They found that a linear relationship held for zonally eastward electric fields using these two sources for a range of values from −0.2 to 1.0 mV/m. To compare the CHAMP and JULIA data, however, correction of ν_{en} by a factor of 4 was needed, just as found by *Gagnepain et al.* [1977]. Details of the procedure to obtain electric field estimates with CHAMP data are described by *Alken and Maus* [2010a]. *Anderson et al.* [2002] use a similar method to determine the electric field using ground magnetometers. They implicitly used the same arbitrary change in ν_{en} when calibrating using the JULIA radar.

[4] Here we report on new numerical modeling that we feel explains a long-standing problem with the altitude of the EEJ. Using the field line–integrated electrodynamics first developed by *Haerendel and Eccles* [1992], we can explain that using an arbitrary constant scaling factor of 4 in the electron-neutral collision frequency is unnecessary. Unlike previous approaches that resolved this discrepancy using an anomalous collision frequency due to plasma waves [*Alken and Maus*, 2010b; *Ronchi et al.*, 1989], our model is classical and does not appeal to a nonlinear plasma instability process to explain the observations.

2. A Classical Resolution to the EEJ Problem

[5] To our knowledge, the only theoretical EEJ work involving field line–integrated quantities was carried out by *Haerendel and Eccles* [1992]. Unfortunately, their earliest calculation was at 17:00 LT since they were studying the prereversal enhancement in the zonal electric field [*Kelley et al.*, 2009]. Nonetheless, they found that the vertical electric field peaked at 107 km without needing to modify the collision frequency. They also found that the field line–integrated Hall conductivity peaked above 105 km, whereas

[1]Department of Electrical and Computer Engineering, Cornell University, Ithaca, New York, USA.
[2]Space Environment Corporation, Providence, Utah, USA.

0148-0227/12/2011JA017020

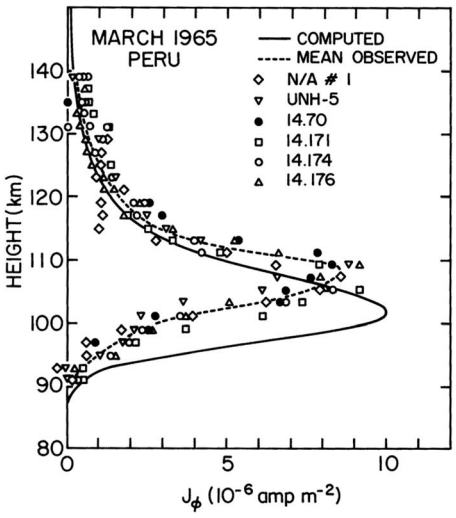

Figure 1. Measurements and theoretical prediction of the eastward current density profile near noon at the equator. The various symbols correspond to rocket designators (see original work by *Davis et al.* [1967], *Maynard* [1967], and *Shuman* [1970]). After *Richmond* [1973], reproduced with permission from Elsevier.

the local value of the Hall conductivity peaked near 103 km. Their electron densities were lower than at noon where the rocket data were obtained, but the density profile shape was very similar to the noontime case, for example, as reported by *Pfaff et al.* [1997]. The latter authors found a peak in the vertical electric field (E_L) and the current density (J) at 105 km, the latter being quite similar to the data in Figure 1. Thus, it is clear that classical local conductivities do not model the EEJ correctly.

[6] Figure 2 (left) shows the local conductivities for a typical period, which are similar to those of *Richmond* [1973] and are based on predictions of the electrical properties of the equatorial ionosphere obtained from the Ionospheric Conductivity Model (ICM), published by the World Data Center (WDC) for Geomagnetism at Kyoto University (available online at http://swdcwww.kugi.kyoto-u.ac.jp/ionocond/sigcal/index.html). This model uses the International Reference Ionosphere (IRI2007) model [*Bilitza*, 2001] for the ionized atmosphere, the MSIS86 model [*Hedin*, 1987] for parameters of the neutral atmosphere, and the collision frequency expressions available from *Banks and Kockarts* [1973].

[7] Figure 2 (right) shows the field line–integrated Hall and Pedersen conductivities. The field line–integrated Hall conductivity, also deduced from the ICM, peaks at a higher altitude than the local values, as also indicated by *Haerendel and Eccles* [1992]. At first, it seems strange that field line integration should matter at such low altitudes, but the nearly horizontal field lines are so long that even a few kilometers of altitude make the integration path sufficiently long enough to matter. As an aside and analogously, the introduction of field line–integrated quantities by Haerendel [*Sultan*, 1994] showed that the altitude range of instability for equatorial spread F was displaced upward to heights above the F peak. This field line–integrated formalism is

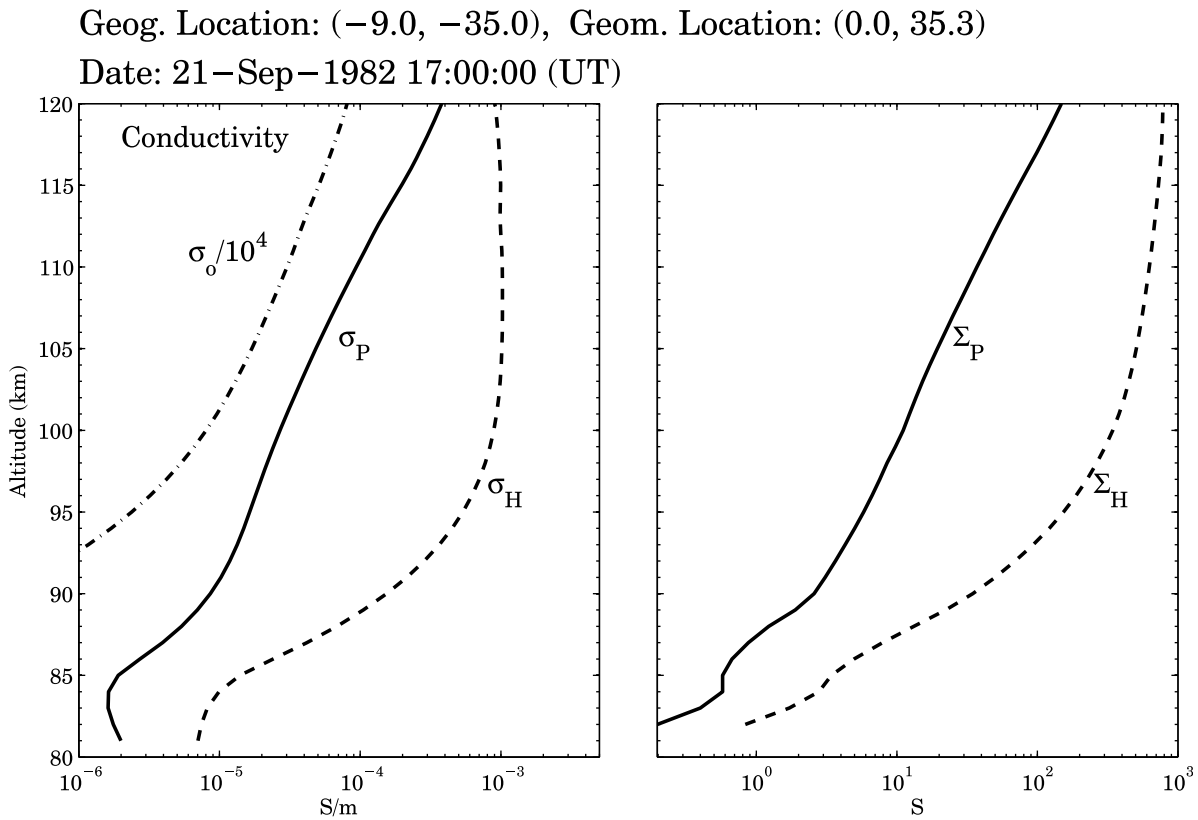

Figure 2. Vertical profile of (left) the local and (right) field line–integrated conductivities at the dip equator on 21 September 1982.

now standard in the spread F field [*Retterer*, 2005]. We believe that the results shown below might have a similar effect on two-dimensional EEJ models.

[8] To adequately test this idea, we have applied the *Haerendel and Eccles* [1992] model to reproduce magnetic field measurements and the inferred currents made by rockets. The local Pedersen and Hall conductivities, σ_P and σ_H, can be represented using the ionic and electronic mobility contributions,

$$\sigma_P = \frac{en}{B}(\mu_{P_i} - \mu_{P_e}),$$
$$\sigma_H = \frac{en}{B}(\mu_{H_e} - \mu_{H_i}),$$

where e is the charge on an electron and has a positive sign, and where the Pedersen and Hall mobilities for ions and electrons are defined as

$$\mu_{P_{i,e}} = \frac{\kappa_{i,e}}{1+\kappa_{i,e}^2},$$
$$\mu_{H_{i,e}} = \frac{\kappa_{i,e}^2}{1+\kappa_{i,e}^2}.$$

The mobility depends on the ratio of the gyrofrequency to the collision frequency, $\kappa_{i,e} = \Omega_{i,e}/\nu_{i,e-n}$, where $\Omega_{i,e} = q_{i,e}B/m_{i,e}$ is the gyrofrequency of the plasma component and has the same sign as $q_{i,e}$. The perpendicular current densities, J_ϕ and J_L, are expressed in a coordinate system that is oriented with respect to the magnetic field, with $\hat{b}$ the unit vector along $\vec{B}$, $\hat{l}$ transverse to $\hat{b}$ in the meridional plane, and $\hat{\phi}$ transverse to both $\hat{b}$ and $\hat{l}$ with $\hat{\phi} = \hat{b} \times \hat{l}$. From integration of the local perpendicular current, the field line–integrated current equations are

$$J_L = \Sigma_P E_L - \Sigma_H E_\phi, \tag{1}$$

$$J_\phi = \tilde{\Sigma}_P E_\phi + \Sigma_H E_L, \tag{2}$$

Σ_P and $\tilde{\Sigma}_P$ are the integrated Pedersen conductivity with different weighting functions, and Σ_H represents the integrated Hall conductivity. These are defined as

$$\Sigma_P = 2R_E L \int_0^{\zeta_m} \sigma_P (1+3\zeta^2) d\zeta, \tag{3}$$

$$\tilde{\Sigma}_P = 2R_E L \int_0^{\zeta_m} \sigma_P d\zeta, \tag{4}$$

$$\Sigma_H = 2R_E L \int_0^{\zeta_m} \sigma_H (1+3\zeta^2)^{\frac{1}{2}} d\zeta, \tag{5}$$

where $\zeta = \sin(\lambda)$ with λ as the dipole latitude. The limits of integration are determined from the ζ value at the equator (0) and at the bottom of the ionosphere (75 km). The factor of 2 in equations (3)–(5) implies symmetry between hemispheres. If equation (1) is solved for E_L and inserted in equation (2), the relations

$$E_L = \frac{J_L + \Sigma_H E_\phi}{\Sigma_P}, \tag{6}$$

$$J_\phi = \Sigma_C E_\phi + \frac{\Sigma_H}{\Sigma_P} J_L, \tag{7}$$

are obtained. Σ_C is the Cowling conductivity defined from integral quantities

$$\Sigma_C = \tilde{\Sigma}_P + \frac{\Sigma_H^2}{\Sigma_P}.$$

The horizontal electric field (E_ϕ) is taken as a given quantity to solve the continuity equation because ionospheric currents are not easily measured whereas electric fields are. If the current continuity equation is integrated over the whole altitude range of the E region, we obtain the local current (A/m) out of or into this region as a result of the EEJ current divergences. This result can be written as the time-dependent quantity

$$\frac{J_L(t) = I_\phi(0) - I_L(t) - \Delta h_E \hat{\Sigma}_C(t) E_\phi(t)}{\Delta h_E \hat{r}_{HP}(t),} \tag{8}$$

where $I_L(t)$ is the vertical current at local solar time t and $I_\phi(0)$ is the initial total horizontal current (t = 0). $\hat{\Sigma}_C(t)$ and $\hat{r}_{HP}(t)$ are the averages of the Cowling conductivity and the ratio of the Hall to Pedersen conductivities, respectively, at the same field line. The latter quantities are expressed as follows

$$\hat{\Sigma}_C(t) = \frac{1}{\Delta h_E} \int_{75km}^{150km} \Sigma_C(t) dh \tag{9}$$

$$\hat{r}_{HP}(t) = \frac{1}{\Delta h_E^2 \Sigma_C(t)} \int_{75km}^{150km} \frac{\Sigma_H(t)}{\Sigma_P(t)} \int_{75km}^{h} \Sigma_C(t) dz dh \tag{10}$$

For simplification, Δh_E = 150 − 75 km is assumed to be the E region altitudinal range. Since E_ϕ is taken as the typical quiet time zonal electric field at noon on the basis of Jicamarca radar measurements [*Kelley et al.*, 2009], it is possible to calculate E_L by using the field line–integrated conductivities (equations (3) to (5)) together with the vertical current density (equation (8)) in equation (6). Note that we arbitrarily take t = 0 at local (solar time) noon. The local current density profiles, j_ϕ and j_L, can be computed by combining the typical zonal electric field (E_ϕ) and the deduced E_L from equation (6) using the local conductivity profiles

$$j_L = -\sigma_H E_\phi + \sigma_P E_L, \tag{11}$$

$$j_\phi = \sigma_P E_\phi + \sigma_H E_L. \tag{12}$$

[9] Figure 3 shows the altitude and magnitude of several parameters, including the horizontal current for 13:00, 14:00, and 15:00 LT on 21 September 1982. This was the quiet period studied by *Haerendel and Eccles* [1992]. Their results were obtained using electron density profiles measured during the Colored Bubbles Experiment [*Haerendel et al.*, 1983], reproduced in Figure 4, and are very similar to our version of this model. The results presented in Figures 3 and 5 are generated by integrated quantities calculated using the International Reference Ionosphere IRI1991 empirical model. We are quite confident that the Haerendel and Eccles model driven by the empirical model is correct.

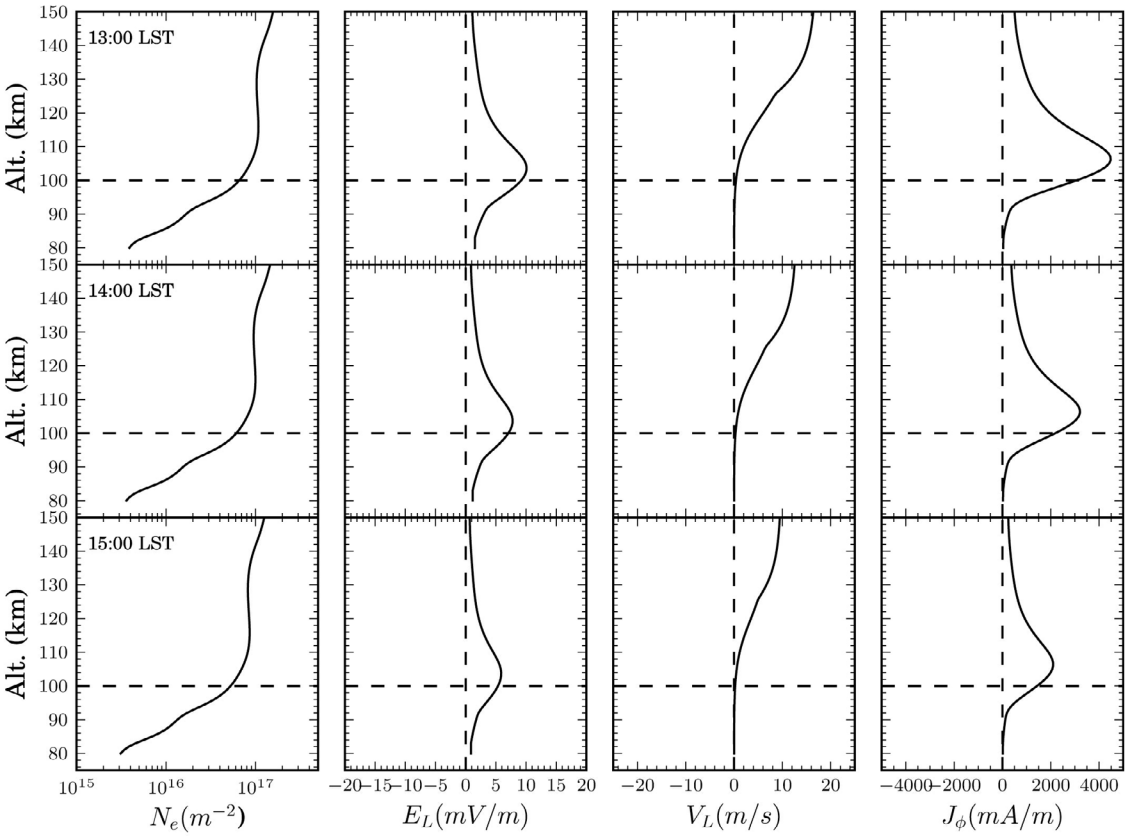

Figure 3. Simulation results for altitude variations in integrated density, vertical electric field, vertical velocity, and horizontal current density for 13:00, 14:00, and 15:00 LT on 21 September 1982. These results use the IRI1991 model as input.

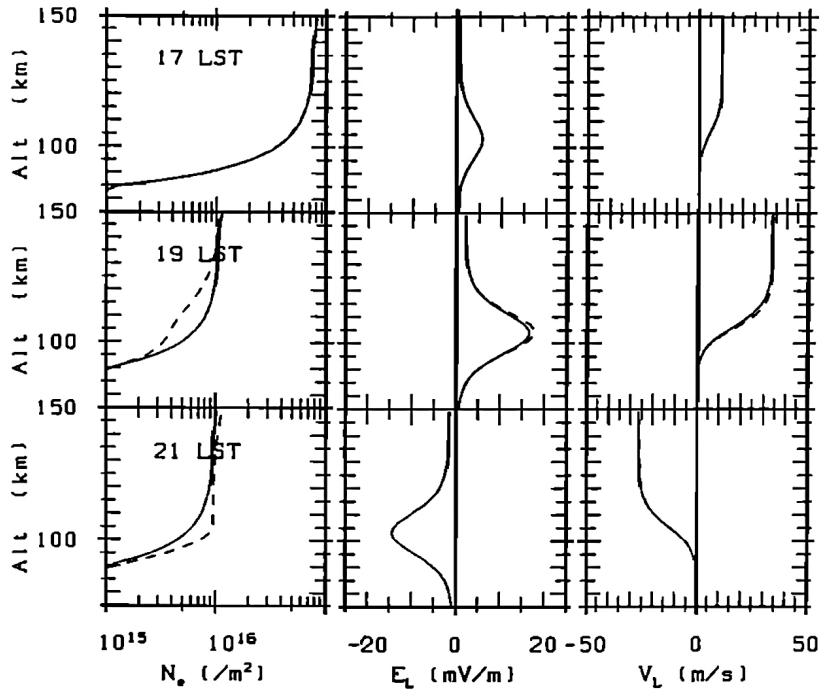

Figure 4. Haerendel and Eccles' results for the same day as in Figure 3 (except J_ϕ) but using measured quantities on that day. The solid curves indicate the model results without dynamics included (the results shown in Figure 3 are obtained with this model configuration). Simulations that include ionization transport are plotted with dashed curves. After *Haerendel and Eccles* [1992].

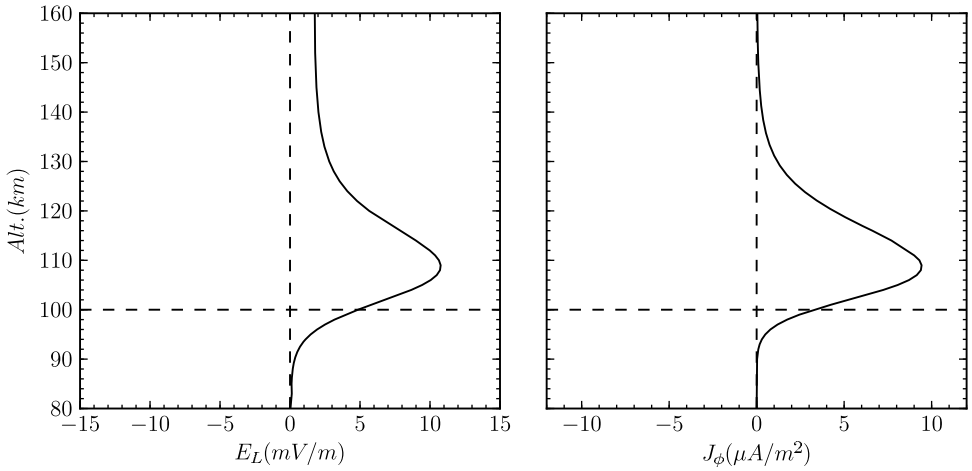

Figure 5. Simulation results for altitude variations in vertical electric field and horizontal current density at the equator for 11:00 LT on 21 September 1994, the day of the *Pfaff et al.* [1997] rocket flight.

This model uses the classical collision frequency and reproduces the observed EEJ altitude quite well. In Figure 5, we use this model to calculate the vertical electric field and the horizontal current density at the magnetic equator on the same day (14 September 1994) as measured by rocket instruments [*Pfaff et al.*, 1987]. The simulated and measured current density (Figure 5) both peak at 109 km, indicating that the *Haerendel and Eccles* [1992] model is in excellent agreement with experiments.

3. Summary

[10] From published rocket measurements of the magnetic field in equatorial electrojet data and numerical simulation results, we find the following.

[11] 1. The long-standing discrepancy between in situ magnetic field observations and theory during quiet conditions can be explained classically if, instead of using local conductivities, field line–integrated values are used.

[12] 2. Prior to this study, the discrepancy in quiet times was attributed to an enhanced electron-neutral collision frequency due to the gradient drift instability. However, it seems that the anomalous collision frequency enhancement by a factor of 4 is a constant from near-zero zonal electric fields to 1 mV/m. The latter point is made since it would be curious if the anomalous collision frequency effect were independent of the driving electric field. We conclude, contrary to previous papers [e.g., *Alken and Maus*, 2010b], that classical collisions adequately explain the observations.

[13] 3. These results do not contradict the idea that for large electric fields, ν_{en} can be increased because of the Farley-Buneman instability [*Ilma et al.*, 2008; *Alken and Maus*, 2010b]. This situation of large electric fields stimulates an instability that is quite different from that of *Ronchi et al.* [1989].

[14] **Acknowledgments.** This work was supported by the National Science Foundation under grant ATM-0551107. The authors also thank Robert Pfaff (GSFF) for providing rocket data and the WDC of Kyoto for making its conductivity model available on the Internet.

[15] Robert Lysak thanks the reviewers for their assistance in evaluating this paper.

References

Alken, P., and S. Maus (2007), Spatio-temporal characterization of the equatorial electrojet from CHAMP, Orsted, and SAC-C satellite magnetic observations, *J. Geophys. Res.*, *112*, A09305, doi:10.1029/2007JA012524.

Alken, P., and S. Maus (2010a), Electric fields in the equatorial ionosphere derived from CHAMP satellite magnetic field measurements, *J. Atmos. Sol. Terr. Phys.*, *72*, 319–326, doi:10.1016/j.jastp.2009.02.006.

Alken, P., and S. Maus (2010b), Relationship between the ionospheric eastward electric field and the equatorial electrojet, *Geophys. Res. Lett.*, *37*, L04104, doi:10.1029/2009GL041989.

Anderson, D., A. Anghel, K. Yumoto, M. Ishitsuka, and E. Kudeki (2002), Estimating daytime vertical $\mathbf{E} \times \mathbf{B}$ drift velocities in the equatorial *F* region using ground-based magnetometer observations, *Geophys. Res. Lett.*, *29*(12), 1596, doi:10.1029/2001GL014562.

Banks, P. M., and G. Kockarts (1973), *Aeronomy*, Academic, London.

Bilitza, D. (2001), International Reference Ionosphere 2000, *Radio Sci.*, *36*(2), 261–275.

Davis, T. N., K. Burrows, and J. D. Stolarik (1967), A latitude survey of the equatorial electrojet with rocket-borne magnetometers, *J. Geophys. Res.*, *72*, 1845–1861, doi:10.1029/JZ072i007p01845.

Gagnepain, J., M. Crochet, and A. D. Richmond (1977), Comparison of equatorial electrojet models, *J. Atmos. Sol. Terr. Phys.*, *39*, 1119–1124.

Haerendel, G., and J. V. Eccles (1992), The role of the equatorial electrojet in the evening ionosphere, *J. Geophys. Res.*, *97*, 1181–1192.

Haerendel, G., O. H. Bauer, S. Cakir, H. Foeppl, E. Rieger, and A. Valenzuela (1983), Colored bubbles: An experiment for triggering equatorial spread *F*, *Eur. Space Agency Spec. Publ., ESA SP-195*, 295–298.

Hedin, A. E. (1987), MSIS-86 thermospheric model, *J. Geophys. Res.*, *92*, 4649–4662, doi:10.1029/JA092iA05p04649.

Ilma, R. R., M. C. Kelley, and J. L. Chau (2008), Intense stormtime equatorial electric fields and evidence for anomalous resistivity in the electrojet, paper presented at 12th International Symposium of Equatorial Aeronomy, Natl. Sci. Found., Crete, Greece, May 18–24.

Kelley, M. C., R. R. Ilma, and G. Crowley (2009), On the origin of prereversal enhancement of the zonal equatorial electric field, *Ann. Geophys.*, *27*, 2053–2056, doi:10.5194/angeo-27-2053-2009.

Maynard, N. C. (1967), Measurements of ionospheric currents off the coast of Peru, *J. Geophys. Res.*, *72*, 1863–1875, doi:10.1029/JZ072i007p01863.

Pfaff, R. F., M. C. Kelley, E. Kudeki, B. G. Fejer, and K. D. Baker (1987), Electric field and plasma density measurements in the strongly driven daytime equatorial electrojet: 2. Two-stream waves, *J. Geophys. Res.*, *92*, 13,597–13,612, doi:10.1029/JA092iA12p13597.

Pfaff, R. F., M. H. Acuña, P. A. Marionni, and N. B. Trivedi (1997), DC polarization electric field, current density, and plasma density measurements in the daytime equatorial electrojet, *Geophys. Res. Lett.*, *24*, 1667–1670, doi:10.1029/97GL01536.

Retterer, J. M. (2005), Physics-based forecasts of equatorial radio scintillation for the Communication and Navigation Outage Forecasting System (C/NOFS), *Space Weather*, *3*, S12C03, doi:10.1029/2005SW000146.

Richmond, A. D. (1973), Equatorial electrojet—I. Development of a model including winds and instabilities, *J. Atmos. Terr. Phys.*, *35*, 1083–1103.

Ronchi, C., P. L. Similon, and R. N. Sudan (1989), A nonlocal linear theory of the gradient drift instability in the equatorial electrojet, *J. Geophys. Res.*, *94*, 1317–1326, doi:10.1029/JA094iA02p01317.

Shuman, B. M. (1970), Rocket measurement of the equatorial electrojet, *J. Geophys. Res.*, *75*, 3889–3901, doi:10.1029/JA075i019p03889.

Sultan, P. J. (1994), Chemical release experiments to induce *F* region ionospheric plasma irregularities at the magnetic equator, Ph.D. thesis, Boston Univ., Boston, Mass.

V. Eccles, Space Environment Corporation, 221 N. Gateway Dr., Ste. A, Providence, UT 84332, USA.

R. R. Ilma and M. C. Kelley, Department of Electrical and Computer Engineering, Cornell University, 318 Rhodes Hall, Ithaca, NY 14853, USA. (mck13@cornell.edu)